

Evaluation and Modeling of Autonomous Attitude Thrust Control for the Geostationary Operational Environmental Satellite (GOES)-8 Orbit Determination*

W. Forcey and C. R. Minnie
Computer Sciences Corporation
Lanham-Seabrook, Maryland, USA

R. L. DeFazio
Goddard Space Flight Center
Greenbelt, Maryland, USA

Abstract

The Geostationary Operational Environmental Satellite (GOES)-8 experienced a series of orbital perturbations from autonomous attitude control thrusting before perigee raising maneuvers. These perturbations influenced differential correction orbital state solutions determined by the Goddard Space Flight Center (GSFC) Goddard Trajectory Determination System (GTDS). The maneuvers induced significant variations in the converged state vector for solutions using increasingly longer tracking data spans. These solutions were used for planning perigee maneuvers as well as initial estimates for orbit solutions used to evaluate the effectiveness of the perigee raising maneuvers.

This paper discusses models for the incorporation of attitude thrust effects into the orbit determination process. Results from definitive attitude solutions are modeled as impulsive thrusts in orbit determination solutions created for GOES-8 mission support. Due to the attitude orientation of GOES-8, analysis results are presented that attempt to absorb the effects of attitude thrusting by including a solution for the coefficient of reflectivity, C_R . Models to represent the attitude maneuvers are tested against orbit determination solutions generated during real-time support of the GOES-8 mission.

The modeling techniques discussed in this investigation offer benefits to the remaining missions in the GOES NEXT series. Similar missions with large autonomous attitude control thrusting, such as the Solar and Heliospheric Observatory (SOHO) spacecraft and the INTELSAT series, may also benefit from these results.

Introduction

The Geostationary Operational Environmental Satellite (GOES)-8 spacecraft was launched on April 13, 1994, at 06:04:02 Universal Time Coordinated (UTC). The nominal maneuver plan called for a series of six orbital maneuvers to place the spacecraft on-station in geosynchronous orbit. The first three of these maneuvers were designed to place the spacecraft in its approximate geosynchronous orbit by increasing the perigee height. Each maneuver, scheduled to be performed at apogee, are called apogee motor firings (AMF). The remaining three maneuvers, the apogee adjust maneuver (AAM) and dual trim motor firings (TMF), produced final corrections to circularize the orbit and place GOES-8 at its assigned longitude.

Actual mission support deviated from the intended nominal maneuver plan. During AMF-1, a maneuver abort was called because of excessive flange temperatures on the main satellite thruster (MST). Subsequently, a new sequence of 5 AMF maneuvers was developed for the transfer phase. The only difficulty with this scenario occurred during AMF-3, when a premaneuver abort was called due to problems with the Attitude and Orbital Control Electronics (AOCE) system, a subsystem responsible for the autonomous control of the attitude.

The MST used for AMF thrusting is part of the GOES Attitude and Orbit Control System (AOCS). The AOCS includes 12 attitude control thrusters, paired throughout the spacecraft, to provide maneuverability in the pitch, roll, and yaw directions. Figure 1 provides a graphical representation of the attitude control thruster locations. The attitude thrusters in Figure 1 represent thruster pairs designed to rotate the spacecraft around a specific body axis (2/3, yaw; 4/5, pitch; 6/7, roll).

* This work was supported by the National Aeronautics and Space Administration (NASA) Goddard Space Flight Center (GSFC), Greenbelt, Maryland, under Contract NAS 5-31500.

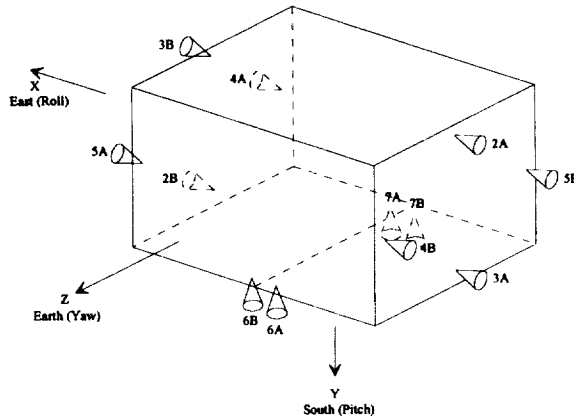


Figure 1. GOES-8 AOCS Attitude Thruster Configuration

In the GOES-8 ascent phase, closed-loop attitude control is performed exclusively with thrusters as actuators. Attitude control is monitored through gyro and sensor output. A particular attitude maneuver is accomplished by an uplink command with unbalanced outputs; the AOCS responds to these offsets by initiating attitude thrust control to match the offset configuration. Once the GOES-8 spacecraft arrived on-station, control of these processes converted from thruster control to momentum wheel control.

Before each AMF maneuver during the ascent phase, attitude control thrusting was completed to configure the spacecraft for the subsequent maneuver. This control thrusting served a number of purposes, most important to 3-axis stabilize the spacecraft and orient the MST for proper delta-V placement during orbit maneuvers. These attitude maneuvers were performed at much smaller thrust levels than the AMF series of maneuvers. Ideally, these maneuvers would incur no net effects on the orbital trajectory, provided thruster pairs operated with balanced force levels and exact alignment. In reality, however, the thrusters are not perfectly balanced, and some misalignment occurs, producing orbital perturbations. This paper describes the best method to treat these autonomous maneuvers for the GOES-8 spacecraft.

The attitude “control box” is defined as the closed-loop tolerance for autonomous attitude control enlisted for a particular orientation. The size of the control box is dependent on the particular mode of attitude control and the requirements for certain sensors. For GOES-8, the control box size was considered large; in fact, real-time support encountered error margins within the same order of magnitude as the size of the control box. In Table 1, the control box sizes are presented referenced to the orientation of the body axes.

Table 1. GOES-8 Attitude Control Box Limits

Attitude Mode	Pitch (deg)	Roll (deg)	Yaw (deg)
Sun Acquisition	+/- 3.00	-	+/- 3.00
Roll Earth Acquisition	+/- 3.00	+/- 0.50	+/- 3.00
Pitch Earth Acquisition	+/- 1.00	+/- 0.50	+/- 1.00
Stationkeeping Mode	+/- 0.25	+/- 0.25	+/- 0.25

The results from real-time orbit determination support of the GOES-8 mission indicate that low-thrust forces did exist due to autonomous attitude control. These perturbations affected orbital state solutions and induced variations in the predicted spacecraft ephemerides for a sequence of solutions that were generated as the satellite approached the next orbit maneuver. The effects of autonomous attitude control are inherently difficult to model, given the imprecise nature of the timeline of events. The concepts included in this analysis evolve into separate topics to discuss possible models: (1) the dynamic representation of these effects by solving for the coefficient of solar radiation pressure and (2) the representation of discrete attitude maneuvers with impulsive thrusts.

Nominal Orbit Determination Results

Orbit determination support for the GOES-8 mission was provided by the Flight Dynamics Facility (FDF) at Goddard Space Flight Center (GSFC). The nominal support scenario for the transfer phase called for a series of the Goddard Trajectory Determination System (GTDS) batch least squares differential correction (DC) solutions to be generated before and following AMF maneuver. Each solution solved only for the epoch state vector. In the hour before an AMF maneuver was to begin, a DC solution termed the best estimated trajectory (BET) was completed to determine the most accurate orbital state before AMF burn ignition. The BET is used as an a priori for AMF thrust estimation solutions (discussed in detail later in this paper) immediately following a maneuver. The methodology involving thrust estimation yields the best available initial state estimate for postmaneuver recovery solutions. The BET solution is also employed as a tool for postmaneuver recalibration of maneuver planning products generated for each orbit maneuver. With these applications in mind, the BET accuracy is considered vital to the general support provided around orbit maneuvers. The orbital states created with the BET are also expected to have stabilized before AMF ignition. This stabilization did not occur during actual mission support; orbital state solutions leading up to a particular AMF maneuver showed significant variations approaching the formulation of the BET. It was theorized that the attitude maneuvers were the cause for this condition.

To illustrate this premise, orbit determination solutions for two premaneuver AMF cases were generated using range and Doppler observations from several tracking stations. The first case, AMF-2, was chosen due to the increase in premaneuver attitude activity prompted by the AMF-1 abort. The second case, AMF-4, was selected because this maneuver had the largest delta-V burn magnitude. In periods before these AMF maneuvers, successive orbital state solutions were completed to furnish updated vectors for acquisition data in support of the National Aeronautics and Space Administration (NASA) and Deep Space Network (DSN) antennae and to provide the foundation for maneuver planning. These series of orbital state solutions exhibited the trends suggesting an increase in attitude control thrusting activity.

The noticeable trends relating to the possibility of attitude control thrusting include increases in solve-for semimajor axis (SMA) values and large differences in ephemeris comparisons for overlapping definitive solutions. In Table 2, both parameters are presented for AMF-2 and AMF-4. The epochs for all solutions were placed near the end of the tracking data span of the specific solution. The designations for solutions (i.e., A8, P15) represent the naming conventions for each segment of the GOES mission; "A" represents the segment before AMF-2 ignition, and "P" represents the phasing orbit segment before AMF-4 ignition. The numerical values represent successive updates in the orbital state determination as a function of time.

Table 2. GOES-8 AMF Premaneuver Orbital State Solution Characteristics

Solution Name	Epoch	Δ SMA (m) at epoch	Stan. Dev. of solved-for SMA (m)	Maximum ephemeris comparison difference (m)
AMF-2				
A8	940418 : 0400	298.7	0.1492	
				5,635.3
A9	940418 : 1600	-17.5	0.4336	
				3,723.3
BET	940418 : 2220	80.3	0.2768	
AMF-4				
P15	940422 : 1900	-6.9	0.3810	
				5,032.3
P17	940423 : 0800	35.4	0.2708	
				3,742.2
P19	940423 : 1439	213.5	0.5038	
				2,824.9
BET	940423 : 1708	272.9	2.3481	

For both AMF-2 and AMF-4, the solution characteristics for the SMA and ephemeris comparisons do not stabilize as the tracking data spans approach the ignition time. Instead, AMF-2 delta SMA values at the epochs vary by as much as 300 meters (m), while maintaining a maximum definitive ephemeris consistency of 3,700 to 5,700 m. The same is true for AMF-4, as delta SMA values increase with solutions approaching burn ignition and definitive ephemeris comparisons range from 2,800 to 5,000 m. The consistent rise in SMA is counterintuitive to the effects of normal perturbative forces (i.e., atmospheric drag, solar radiation pressure), prompting the notion that an unmodeled perturbative force was influencing the solution quality. The

random nature of delta SMA values for AMF-2 and the ephemeris comparisons for AMF-4 implies that the perturbative force varied in magnitude throughout the timespans represented in the solutions, leading to the idea that autonomous attitude control thrusting is the possible source for these irregular trends.

To confirm the effects of attitude control thrusting, a definitive outline of AMF-2 premaneuver attitude control events was compiled. Attitude events were culled from mission support for the 6-hour period leading up to AMF-2 ignition and including the initial period following the completion of the maneuver. In Table 3, the largest attitude control events are listed, noting the orientation affected and the purpose of the maneuver.

Table 3. GOES-8 Pre-AMF-2 Attitude Control Maneuvers

Maneuver	Time (UTC)	Description
1	4/18/94, 18:08:00	DSS Pitch Bias : Capture Earth while maintaining sun sensor coverage
2	4/18/94, 18:53:00	DSS Yaw Bias Command : Cool MST thruster flange temperatures
3	4/18/94, 19:55:00	DSS Pitch Bias Command : Maintain Earth coverage through calibrations
4	4/18/94, 20:39:00	Pitch Earth acquisition
5	4/18/94, 22:06:00	Yaw Reorientation : Ensure AMF-2 delta-V in correct direction
-	-	Stationkeeping Mode : High thruster activity
6	4/18/94, 22:34:00	AMF-2 commences
-	-	Sun Acquisition : Return to normal Sun acquisition mode

DSS = digital Sun sensor

The attitude control thrusting outlined in Table 3 reflects possible events that could influence orbital state solutions. While only discrete events are listed, the effects of stationkeeping within a 0.25 deg control box cannot be neglected. To enhance the representation of the events listed in Table 3, Figure 2 depicts the relative position of these events in the GOES orbital plane, based on true anomaly. This figure also shows the orientation of the Sun and spacecraft. The -X axis is generally in the direction of the Sun and the +Z axis is generally in the direction of the Earth. The event designations correlate with the listing provided in Table 3.

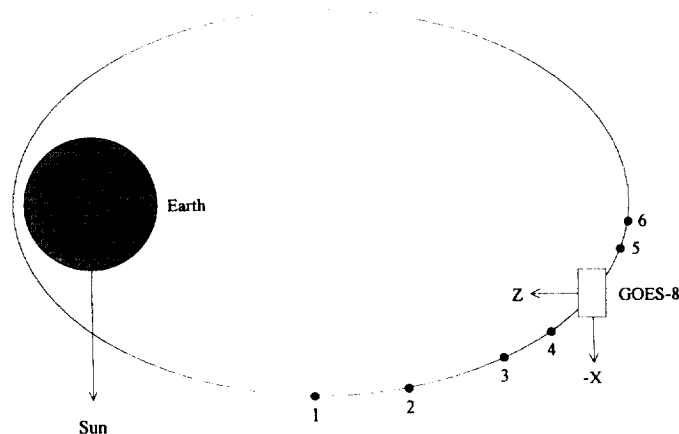


Figure 2. Representation of GOES-8 Attitude Maneuvers Within the Orbital Plane Frame of Reference

The discrete events listed in Table 3 should be visible through the examination of residuals from the DC process. These residuals would reflect instantaneous perturbative effects from range and/or range rate tracking system measurements, ruling out equipment anomalies. The strongest indication of attitude control events came from range rate residuals generated within

the BET solution. In Figure 3, the residuals for the final iteration of the BET definitive period before AMF-2 are presented for range rate tracking data measurements from the DS61 (Madrid) 34-meter DSN site. The a priori vector for this DC solution was provided by the A9 solution, created less than 2 hours before the BET. Figure 3 represents only a portion of the tracking data included for the BET solution. Additional tracking data were received from other sites, but this portion was chosen due to the clear representation of attitude effects.

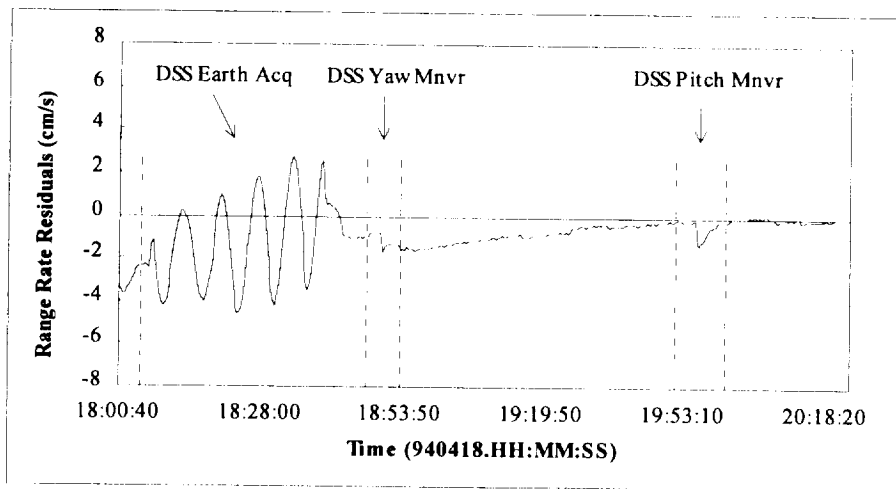


Figure 3. GOES-8 Pre-AMF-2 Final Iteration Range Rate Residuals From Madrid (Nominal Solution)

Within the timeframe provided by the DS61 tracking data pass, the distinct effects of three attitude control maneuvers are recognized. Each residual disturbance apparent in Figure 3 correlates to an attitude control maneuver as outlined in Table 3. The first maneuver, the DSS Earth Acquisition, is a series of small burns performed to stabilize the spacecraft in 3-axis mode through Earth acquisition, hence the periodic motion of the residuals as the spacecraft oscillates in pitch. The last two maneuvers, the DSS Yaw Bias and the DSS Pitch Bias, perform secular rotations for the purposes summarized in Table 3. Because of the lack of tracking data over the period encompassing the remaining maneuvers, no residuals were generated for these events. A similar timespan of tracking was simultaneously received from the tracking station at Wallops Island, Virginia. The residuals generated from this tracking data directly correlate to events displayed in Figure 3, ruling out possible anomalies in equipment at the respective tracking stations.

With the results from AMF-2 in mind, a similar procedure was completed for the period before AMF-4. Figure 4 depicts the pre-AMF-4 residual region for the same relative time period as AMF-2. Comparable regions of residual disturbances exist between Figures 4 and 3.

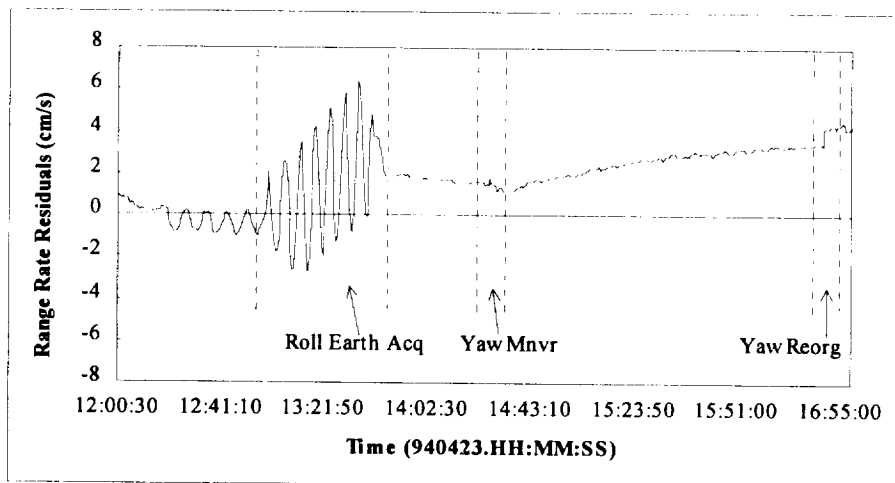


Figure 4. GOES-8 Pre-AMF-4 Final Iteration Range Rate Residuals From Madrid (Nominal Solution)

The residual disturbances found in Figure 4 can be traced to a listing of the confirmed attitude events before AMF-4. Table 4 lists the discrete attitude events that correlate to the occurrences presented in Figure 4. These results establish the constant scenario of attitude control thrusting that has been confirmed for each AMF maneuver.

Table 4. GOES-8 Pre-AMF-4 Attitude Control Maneuvers

Maneuver	Time (UTC)	Description
1	4/23/94, 13:45:36	Roll Earth acquisition complete
2	4/23/94, 14:29:12	Pre-Yaw Maneuver : Cool MST flange
3	4/23/94, 15:34:36	Pitch Earth acquisition
4	4/23/94, 16:54:14	Yaw Reorientation : Place spacecraft in attitude to perform AMF-4 delta-V
5	4/23/94, 16:58:18	Pitch Reorientation : Small burn for pitch orientation
-	-	Stationkeeping Mode : High thruster activity
6	4/23/94, 17:22:58	AMF-4 commences
-	-	Sun Acquisition : Return to normal Sun acquisition mode

The attitude control events presented in Tables 3 and 4 are not the only contributing elements to the overall autonomous attitude control effect. As mentioned previously, the tight attitude control box in place during stationkeeping mode elicits a high degree of attitude thrusting activity. The effects of attitude control are also not limited to the period of time immediately before an AMF maneuver. While not at the same magnitude as pre-AMF activity, attitude thrust control effects were experienced throughout the mission. The effects subsided with the conversion of attitude control to momentum wheels.

With the recognition of autonomous attitude control effects on orbital state solutions comes the question concerning the modeling of these effects. For this analysis, two approaches are assessed: dynamic solar radiation pressure modeling (i.e., solving for C_R) and impulsive thrust modeling.

Orbit Determination Results That Include a Solution for C_R

One possible approach to modeling the perturbative effects of the attitude thrust control is using dynamic solar radiation pressure force modeling. This modeling approach is appropriate for this investigation because GOES-8 attitude is Sun-referenced (Figure 2) and most residual delta-V will be applied along the Sun or anti-Sun pointing vector. The GTDS software includes the capability to solve for C_R in the DC process. The mathematical equation governing the relationship between C_R and the acceleration due to solar radiation pressure is as follows:

$$\ddot{\mathbf{R}}_{SR} = \nu P_s R_{sun}^2 \frac{C_R A_{Ref}}{m} \frac{\bar{\mathbf{R}}_{sv}}{R_{sv}^3} \quad (1-1)$$

where $\ddot{\mathbf{R}}_{SR}$ = acceleration due to solar radiation pressure
 ν = Eclipse factor ($0 < \nu < 1$)
 P_s = Constant (solar flux at 1 AU / speed of light)
 A_{Ref} = Spacecraft cross-sectional area
 m = Spacecraft mass
 R_{sun} = Earth - Sun vector
 R_{sv} = GOES-8 - Sun vector

The solar radiation pressure force acts along the Sun-spacecraft vector. The physical limitations of C_R range from 0 to 2 (with 0 representing a body with no momentum transfer due to photons and 2 representing a completely reflective body). During the early phases of the GOES-8 mission, solving for C_R was avoided due to the relatively high eccentricity of the orbit [$e = 0.738$ (pre-AMF-2)] and the smaller values of SMA. The high eccentricity requires the satellite to travel within two separate regions in which different perturbative forces are significant; at perigee, the satellite experiences a higher magnitude of atmospheric drag, while at apogee, solar radiation pressure is significant. This method does, however, have some advantages. Without the benefit of other solve-for parameters, a solve-for C_R corrects for any and all existing perturbations on the spacecraft that have similar characteristics to that of the force due to solar radiation pressure.

During real-time orbit determination support, modeling of solar radiation pressure was limited to the use of a nominal value of C_R in the integration of the satellite equations of motion. For the GOES mission, this value was determined to be 1.5 (Reference 1). Testing of C_R solve-for solutions commenced with analysis of the AMF-4 premaneuver scenario. The solution scenario presented through results in Table 2 were reevaluated through dynamic solar radiation modeling. In each case, the coefficient of reflectivity was solved for in addition to the orbital state. The resulting ephemeris was then compared to the corresponding nominal ephemeris from mission support as well as common intervals of the prior ephemeris, which solved for C_R . These results appear below in Table 5.

Table 5. GOES-8 Pre-AMF-4 C_R Solve-for Results

Solution	Epoch	C_R	C_R Stan Dev	Maximum Ephemeris Position Difference (m)	
				C_R and Nominal Solutions	Successive C_R Solutions
P15	4/22/94 : 1900	28.049	0.0144	2,564.6	
					3,506.7
P17	4/23/94 : 0800	30.190	0.0276	588.6	
					251.9
P19	4/23/94 : 1200	22.440	0.1280	632.5	
					13,771.5
BET	4/23/94 : 1708	-25.824	0.0670	4,108.9	

From the results in Table 5, the influence of indeterminate perturbative forces outside of solar radiation pressure can be established. The solve-for values of C_R range far above the nominal value of 1.5 and exceed the constraints that define the physical application of the solar radiation effects. To quantify the exact perturbative acceleration attributed to solar radiation pressure, the relationship presented in Equation (1) can be used. Table 6 presents accelerations that were generated using the solve-for values of C_R outlined in Table 5 in conjunction with Equation (1).

Table 6. GOES-8 Accelerations Due to Solar Radiation Pressure for Pre-AMF-4 Solutions

Solution	Solve-for value of C_R	Acceleration from C_R model (m/s^2)
P15	28.049	9.99e-07
P17	30.190	1.07e-06
P19	22.440	8.00e-07
BET	-25.824	9.20e-07

The nominal range of accelerations attributed to solar radiation pressure lies between $5.0e-08$ to $5.0e-09$ m/s^2 (Reference 2), taken from a random distribution of satellite missions previously launched into orbit. The results obtained from solutions created for GOES-8 are at least one full order of magnitude greater than the nominal range. This discrepancy indicates that solving for C_R is compensating for perturbations beyond solar radiation pressure. This is substantiated by premission covariance analysis, in which attitude thrusting was modeled with an acceleration magnitude of approximately $1.45e-06$ m/s^2 (Reference 1). This value, with nominal solar radiation pressure effects included, corresponds to within 20 to 30 percent of the solve-for values for solar radiation pressure force acceleration from real-time mission support. Given the large disparity between predicted and actual values for solar radiation accelerations, the conclusion that attitude effects are distinctly perturbing the orbital trajectory can be established.

A counterpoint to the notion that attitude effects are the primary reason for the large solve-for values of C_R lies in the possible effects of atmospheric drag. Inspection of the orbital elements for the pre-AMF-4 period suggests that drag will not influence the use of C_R . In this phase of the GOES-8 mission, the apogee height was approximately 49,000 km, and the perigee height 13,660 km. Within this region, drag effects are presumed minimal. This assumption was reinforced through tests that solved for the effects of drag.

Beyond the recognition of distinct perturbative effects, the introduction of C_R as a modeling tool for attitude control effects stabilized the results of the DC process in orbit determination solutions. The DC process generates a number of statistics regarding the convergence quality of an orbital state solution. One set of these statistics involves the tracking data residual

quality. For GOES-8, the two major tracking data types were Universal Ranging (URAN) and Universal Range Doppler Format (URDF). In analyzing the standard deviation, σ , and the root-mean-square (RMS) of these residuals, the quality of the respective tracking data fits can be interpreted. In Table 7, the residual standard deviations are presented for the nominal solutions and those that solve for C_R .

Table 7. GOES-8 Tracking Data Residual Standard Deviations for Pre-AMF-4 Orbital State Solutions

Solution	Nominal Solution				C_R Solve-for Solution			
	URAN σ (m)	URAN RMS	URDF σ (cm/s)	URDF RMS	URAN σ (m)	URAN RMS	URDF σ (cm/s)	URDF RMS
P15	04.861	0.228	1.572	0.186	1.604	0.080	0.167	0.017
P17	02.588	0.130	0.944	0.108	1.067	0.083	0.163	0.016
P19	02.890	0.145	0.777	0.078	2.014	0.101	0.336	0.034
BET	22.780	1.134	4.371	0.447	3.798	0.190	0.938	0.094

From the results in Table 7, initial conclusions can be drawn concerning the positive effects of solving for C_R . In each solution, there is a substantial reduction in the standard deviation for the residuals of the respective data types. Standard deviation values for URAN tracking decrease by an average of 60 percent, while the URDF standard deviation values fall by an average of 80 percent. In addition to this study of residual tracking results, some insight can be gained through the analysis of the final orbital state correction produced in the DC process. For each solution leading up to AMF-4 ignition, the difference in the converged orbital state (Cartesian position) between the C_R -modeled and nominal solution increases. These state corrections range in magnitude from 424.3 m for the P15 solution to 4,863.8 m for the BET solution. This suggests an increase in the perturbative effects modeled through the C_R solve-for method. In addition, standard deviation results from the orbit determination solutions reveal improved tracking data fits produced with the C_R solve-for method. Table 8 displays these results for pre-AMF-4 orbit determination solutions.

Table 8. GOES-8 Pre-AMF-4 Orbital State Statistics

Solution	Standard Deviation of Total Position (m)		Reduction in Average Standard deviation (%)
	Nominal Solution	Solve-for C_R Solution	
P15	03.633	01.027	71.731
P17	01.787	01.063	40.487
P19	03.226	02.081	35.484
BET	27.327	13.527	50.500

The results in Table 8 again indicate that a perturbing force is inducing effects on DC solutions. With the assistance of dynamic C_R modeling, the solutions appear to produce a better representation of the observations. Similar results were generated for pre-AMF-2 solutions.

These DC process results can also be analyzed through representation of the tracking data residuals. In Figure 5, the residuals from a dynamic C_R -modeled solution are displayed over approximately the same timespan as Figure 3. As with the nominal orbit determination solutions, only Doppler residuals are presented because they are more sensitive to the attitude maneuvers. One interesting characteristic of Figure 5 is the instantaneous variations that exist in the residuals, most notably during the roll Earth acquisition sequence.

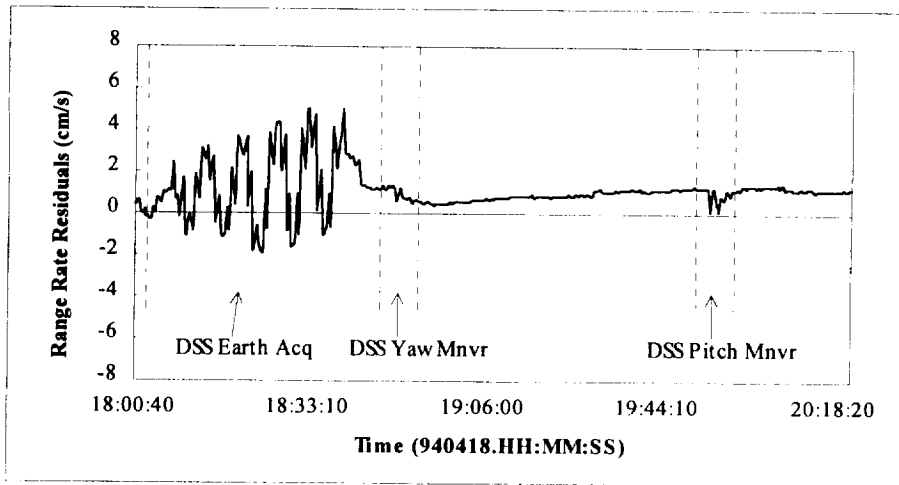


Figure 5. GOES-8 Pre-AMF-2 BET Final Iteration Range Rate Residuals From Madrid (C_R Modeled Solution)

The overall use of dynamic solar radiation pressure modeling has proven to be effective in mitigating the effects of autonomous attitude thruster control for GOES-8. One of the most convincing arguments for its use appeared after the autonomous attitude thruster control ceased. In orbital state solutions following the transition of momentum control to wheels, C_R values stabilized from the 20 to 30 range to steady values in the 1.2 to 1.4 range. These values are comparable to predicted estimates generated during premission analysis (Reference 1).

Orbit Determination Results that Model Attitude Maneuvers as Impulsive Thrusts

Impulsive thrust modeling presents a second possible method for approximating the effects of attitude control thrusting. In this method, discrete events in the series of attitude control maneuvers before the AMF burns are treated as impulsive maneuvers. The impulsive thrust model (ITM) used in GTDS requires the user to define one or more impulsive delta-Vs that are added to the state vector calculated at the maneuver epoch. This process requires knowledge of the attitude of the spacecraft and the orientation of the attitude thrusters relative to the body centered coordinate system shown in Figure 1.

The first test of modeling the attitude maneuvers as impulsive thrusts involved a procedure that simply propagated the state vector from the BET of the nominal solution. This propagation process included adding the impulsive delta-Vs at the appropriate times. This initial test did not involve orbit determination but simply propagation that includes impulsive thrusts to represent attitude maneuvers. This process allows an immediate evaluation of the effects of the approximated attitude maneuvers on the SMA. The delta SMA results from actual orbit determination solutions are presented in Table 2.

This procedure was carried out for both AMF-2 and AMF-4 with the delta-Vs outlined in Tables 3 and 4, with the exception of the roll Earth acquisition sequence. The nature of this specific maneuver should involve modeling with a time history and is, therefore, not appropriately represented by an impulsive thrust. Table 9 presents the results of the changes in several of the Keplerian parameters due to the inclusion of the impulsive representation of the attitude control maneuvers. The values represent Keplerian parameters before the initial modeled attitude maneuver relative to the Keplerian parameters following the completion of the final modeled attitude maneuver.

Table 9. Keplerian Element Variations Due to Impulsive Attitude Events for AMF-2 and AMF-4

Impulse (m/s)	Δ SMA (km)	Δ SMA/SMA	Δ ecc	Δ ecc/ecc	Δ inc (deg)	Δ inc/inc
AMF-2						
10	273.6179	0.0097	-0.0109	-0.0145	-0.0119	-0.0005
1	26.9363	0.0010	-0.0011	-0.0015	0.0049	0.0002
.1	2.7235	9.66e-05	-0.0001	-0.0002	0.0067	0.0003
.01	0.3067	1.09e-05	-3.73e-05	-5.06e-05	0.0068	0.0003
AMF-4						
10	377.3714	0.0120	-0.0144	-0.0255	-0.1239	-0.0111
1	36.8620	0.0012	-0.0015	-0.0026	-0.0134	-0.0012
.1	3.4763	0.0001	-0.0002	-0.0004	-0.0021	-0.0002
.01	0.1443	4.61e-06	-8.50e-05	-0.0002	-0.0010	-8.74e-05

The changes in SMA noted in Table 9 indicate that the attitude control maneuvers produce an orbit-raising effect. This correlates to the information presented in Table 2 from real-time mission support. While the full complement of pre-AMF attitude control maneuvers is not included in the ephemeris created with the impulsive thrusts, the results lead to the conclusion that attitude thrusting can provide changes in the orbital parameters that are comparable to results generated during the GOES-8 mission.

The implementation of this concept would best occur while the BET is being created. With possible attitude effects modeled in this solution, the most accurate orbital state before the orbit maneuver is achieved. However, the concept of autonomous thrust control promises difficulty with implementation of this scheme. As mentioned previously in this paper, the stationkeeping mode immediately before orbit burn ignition produces non-orbit neutral attitude effects that cannot be distinguished discretely.

A better method of representing the attitude maneuvers is to include the impulsive thrusts in the generation of the trajectory that is used to estimate a best-fit orbit state as part of a DC solution. This procedure was applied to the pre-AMF-4 solution. The residuals associated with this solution are shown in Figure 5, over the same time period as presented in Figure 3.

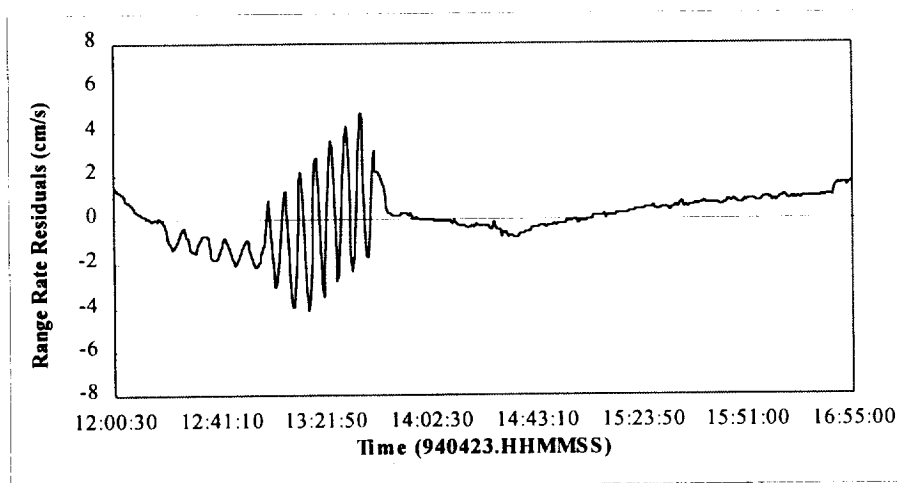


Figure 6. GOES-8 Pre-AMF-4 Final Iteration Range Rate Residuals From Madrid (Impulse Modeling)

In Figure 6, positive effects from the introduction of impulse modeling can be distinguished. There is a clear reduction in the residual size when comparing the results from Figure 6 with those presented in Figure 4. While the unmodeled roll Earth acquisition sequence remains in the same residual magnitude range, the residuals encompassing the modeled attitude maneuvers decrease. Given the use of batch least squares approximations in the DC process, the success of this methodology would appear as a general decrease in the residual magnitudes.

The above discussion has indicated that the use of impulsive modeling can characterize the effects of attitude thrust control. The single drawback to using these methods of representing the attitude maneuvers results from the inability to model the high frequency of autonomous attitude thrusting occurring in the stationkeeping mode.

Thrust Estimation

With analysis completed on several treatments of attitude thrust control, these ideas were implemented for a real time orbit determination scenario. During mission support, one FDF requirement is to provide real-time postmaneuver orbit determination solutions as quickly as possible. Generally, the amount of tracking data available in the allotted period following a maneuver is insufficient to generate accurate orbital states. Two techniques are incorporated to overcome the limitations on the amount of tracking data and the time available to obtain a postmaneuver solution. First, constraints are placed on the a priori values of SMA and mean anomaly. This implies the need for the best possible estimate for the constrained parameters, hence the need for the BET. Second, the GTDS allows for the use of a maneuver thrust model (MTM)

that patterns the effects of an orbit maneuver. Instead of applying an impulsive delta-V, this model incorporates time-dependent nominal accelerations applied to the spacecraft by control thrusters throughout the execution of an orbit maneuver.

During mission support, a General Maneuver Program (GMAN) file is created to represent the nominal thrust acceleration for each AMF maneuver. The GTDS solves for a spacecraft orbital state using tracking data before, during, and after the maneuver with the accelerations due to the maneuver read from the GMAN file. During operational support, the GMAN predicted acceleration file for a particular maneuver is created before the completion of the BET. Therefore, any discrepancies that exist between the BET and the orbital state used to create the GMAN burn file would possibly reflect on the accuracy of thrust estimation.

To estimate differences in the nominal thrust model and that indicated by a solution from tracking data before, during, and after the maneuver period, a perturbative solve-for exists within GTDS modeling capabilities. The thrust coefficient, C_T , is a scaling factor for the nominal thrust model and compensates for disparities that exist between the GMAN burn file and the orbital state corrections reflected by tracking data. Table 10 presents results taken from thrust estimation solutions utilizing a priori vectors created with dynamic C_R models and the nominal support case.

Table 10. Thrust Coefficient Solve-for Values for AMF-2 and AMF-4

A Priori Vector	Thrust Coefficient (C_T)	
	AMF-2	AMF-4
Nominal	-0.01387	-0.006439
C_R	-0.01377	-0.006088

The reduction in C_T for AMF-2 and AMF-4 is 0.72 percent and 5.4 percent. In the process of completing thrust estimation, an ephemeris using the GMAN burn file is created that models the maneuver period. Comparisons were generated using the C_R modeled thrust ephemeris and the nominal thrust ephemeris. For AMF-4, the delta-r value between the ephemerides before the maneuver was nearly constant at 4.1 km, which is approximate to the converged orbital state difference of 4.9 km exhibited between the C_R and nominal DC solution. Postmaneuver comparisons, however, revealed that the delta-r values between the two ephemerides rose to 32 km after 12 hr, and 51 km after 24 hr. These comparisons were repeated for the AMF-2 maneuver scenario; the results revealed a constant premaneuver comparison of 2.5 km, along the same order as the 2.4-km comparison generated in C_R BET testing. The postmaneuver comparisons for AMF-2 reached a magnitude of 6.0 km after 24 hr. These results reveal the effects that small discrepancies in C_T can produce given large-scale delta-v values for AMF maneuvers.

Summary

This paper has analyzed the effect of autonomous attitude control maneuvers on orbit determination of the GOES-8 spacecraft during the early orbit phase of the mission. Neglecting these attitude maneuvers can lead to relatively poor orbit determination results, while attempting to model them is inherently difficult due to the unknown characteristics of many of the individual maneuvers.

The design of the spacecraft and mission resulted in delta-v from attitude maneuvers to lie mostly on the Sun-to GOES-8 vector. This specific feature permits a simplified procedure for modeling the autonomous maneuvers by solving for the coefficient of radiation pressure to help absorb the accelerations due to the maneuvers.

The analysis has been divided into four cases. First, "nominal" orbit solutions have been obtained by ignoring all maneuvers and generating an orbit solution from range and Doppler tracking data from the Madrid, Wallops Island, and Canberra ground sites. Second, orbit solutions have been created from the same tracking data but these include a solution for the coefficient of radiation pressure to help absorb the effects of the attitude maneuvers. Third, orbit solutions have been generated that model most of the autonomous maneuvers as impulsive thrusts. Finally, solutions were generated that assume a finite burn period with a nominal magnitude and direction for a perigee raising maneuver, but they estimate a scale factor for the magnitude of the maneuver.

Conclusions

Attitude maneuvers for the early orbit phase of GOES-8 produced a significant effect on the real-time mission orbit determination solutions. The analysis in this investigation has shown the following characteristics.

Case 1. Solutions that do not model attitude maneuvers (nominal solutions)

- a. A series of solutions leading up to the BET indicate an increase in the converged SMA of the GOES-8 orbit. This suggests the existence of an unmodeled perturbation.
- b. The trends in the residual patterns of these solutions also indicate the existence of an unmodeled perturbation.

Case 2. Solutions that solve for the coefficient of radiation pressure

- c. These solutions produced solved-for values of C_R (20 to 30) that greatly exceed the nominal limits for this parameter (0 to 2). This further substantiates the existence of an unmodeled perturbation.
- d. The standard deviation of the residuals for solutions that solve for C_R are nearly an order of magnitude smaller than for the corresponding nominal solutions in Case 1.
- e. The RMS for the solved-for orbital state components are substantially smaller than those of the nominal solutions.

Case 3. Solutions that model attitude maneuvers as impulsive thrusts

- f. Modeling attitude maneuvers as impulsive thrusts and adding the corresponding instantaneous velocity increments to an orbit propagation (not an orbit determination solution) produced increases in the SMA of the GOES-8 orbit. This further substantiates the idea that the attitude maneuvers produced unmodeled perturbations in the nominal solutions.
- g. Orbit determination solutions that include a modeling of the attitude maneuvers as impulsive thrusts produce the smallest RMS and standard deviation of residuals with no significant deviation from a zero mean.

Case 4. Solutions that solve for the magnitude of the perigee raising maneuver

- h. Comparing thrust-modeled ephemerides based on varying a priori vectors (nominal, C_R) produced sizable position differences that correlated with orbital state correction discrepancies.
- i. Small changes in C_T produced by using C_R -modeled a priori vectors created substantial postmaneuver differences in ephemeris comparisons with nominal thrust solutions.

Recommendations

The results of this investigation suggest that a decision will need to be made concerning which methodology should be endorsed to model autonomous attitude maneuvers for spacecraft with similar characteristics to GOES-8. The best fit to the tracking data results from solutions that model the attitude maneuvers in the orbit determination process. If, however, impulsive thrust modeling is not a software option, then solving for C_R produces a distinct improvement in the orbit solutions for spacecraft with an attitude orientation similar to that of GOES-8. Both techniques render superior orbit fits to solutions that ignore the existence of the attitude maneuvers.

Acknowledgments

The authors would like to thank the following people for their contributions towards the presentation of this paper: Caroline Noonan and John Rowe for information concerning the GOES-8 attitude system and Allan Schanzle for overall technical and presentation review.

References

1. Computer Sciences Corporation, "Report on Error Analysis for the Transfer Orbit Phase of the Geostationary Operational Environmental Satellite (GOES) (memorandum)," A. Schanzle, J. Rovnak, and D. Oza, August 1993
2. Goddard Space Flight Center, Flight Dynamics Division, FDD/552-89/001, *Goddard Trajectory Determination System (GTDS) Mathematical Theory (Revision 1)*, A. C. Long, J. O. Cappellari, C. E. Velez, and A. J. Fuchs, July 1989
3. A. Milani, A. M. Nobili, and P. Farinella, *Non-Gravitational Perturbation and Satellite Geodesy*, A. Hilger, 1987
4. F. P. J. Rimrott, *Introductory Orbit Dynamics*, Vieweg, 1989

